Synthetic dsDNA-Binding Peptides Using Natural Compounds as Model

by **Filip Borgions**, **Daniel Ghyssels**, **A. Van Aerschot**, **J. Rozenski**, and **Piet Herdewijn***

Laboratory of Medicinal Chemistry, Rega Institute for Medical Research, K. U. Leuven, Minderbroedersstraat 10, B-3000 Leuven
(phone: +32-16-337387; fax: +32-16-337340; e-mail: Piet.herdewijn@rega.kuleuven.be)

We have developed a series of short DNA-binding peptides containing newly synthesized, unnatural as well as natural amino acid building blocks. By a combinatorial-library approach, oligopeptides were developed with moderate dsDNA-binding affinities. Two strategies were used to further enhance the binding affinity of the lead peptides: Ac-Arg-Ual-Sar-Chi-Chi-Chi-Arg-NH_2 and Ac-Arg-Cbg-Cha-Chi-Chi-Tal-Arg-NH_2. Site-selective amino acid substitutions increased the binding affinities up to 2×10^{-5} M. Further enhancement of the binding affinities could be achieved by coupling of an acridine intercalating unit, using linker arms of different length and flexibility. With the introduction of a new lysine-based acridine unit, different types of oligopeptide–acridine conjugates were designed using known dsDNA-binding ligands as model compounds. The binding capacities of these new oligopeptide–acridine conjugates have been investigated by a fluorescent intercalator (ethidium bromide) displacement (FID) assay. With the synthesis of the dipeptide–acridine conjugates, binding affinities in the low micromolar range were obtained (6.4×10^{-6} M), which is similar to the binding strength of the well-known DNA binder *Hoechst 33258*.

Introduction. – Since all life processes originate from DNA, the carrier of the genetic information, DNA can be considered as a macromolecular receptor with unlimited possibilities. Antigene agents may be able to manipulate transcription of individual genes and, hence, are potentially useful for the treatment of cancers as well as genetic and infectious diseases [1][2]. During the years, remarkable progress has been made in the design of DNA-targeting drugs, and, more recently, the design of the first molecules capable of *in vivo* regulation of gene expression in a very specific manner [3]. In spite of this success, most approaches are still confronted with problems as aspecific recognition, low ability to penetrate into cells, and even low biological stability [2][4]. Due to the drawbacks of these approaches and the great potential of DNA as a receptor, the search for new dsDNA-binding compounds needs to be continued.

The design of short unnatural oligopeptides capable of binding DNA in analogy with natural DNA-binding proteins is one of the possibilities to search for gene-regulating compounds. The design of short dsDNA-binding peptides also contributes to the understanding of the mechanisms involved in the recognition of dsDNA by proteins and small molecules. Previously, a solution-phase screening of combinatorial libraries consisting of unnatural oligopeptides has resulted in the discovery of dsDNA-binding peptides with affinities in the low millimolar range [5]. In this paper, a further optimization of the potency of these lead peptides is described.

Results and Discussion. – *Optimization of the dsDNA-Binding Affinity by Site-Selective Amino Acid Substitutions.* The oligopeptide Ac-Arg-Ual-Sar-Chi-Chi-Chi-Arg-NH_2, having a K_d value of 2.0×10^{-4} M for a 14-mer dsDNA target as determined by a fluorescent-intercalator displacement (FID) assay, was selected as lead peptide for further optimization (*Fig. 1*). Investigations with glycine-substituted oligopeptide analogues indicated that the interactions of the uracil (Ual) and sarcosine (Sar) side chains contribute less to the overall DNA-binding affinity of the oligopeptide than the quinazoline dione (Chi) side chains [6]. Consequently, the Ual and Sar positions were modified with several new commercially available amino acid building blocks in order to increase the contribution of these positions to the stability of the oligopeptide–DNA complex. Hereto, a parallel synthesis approach was used.

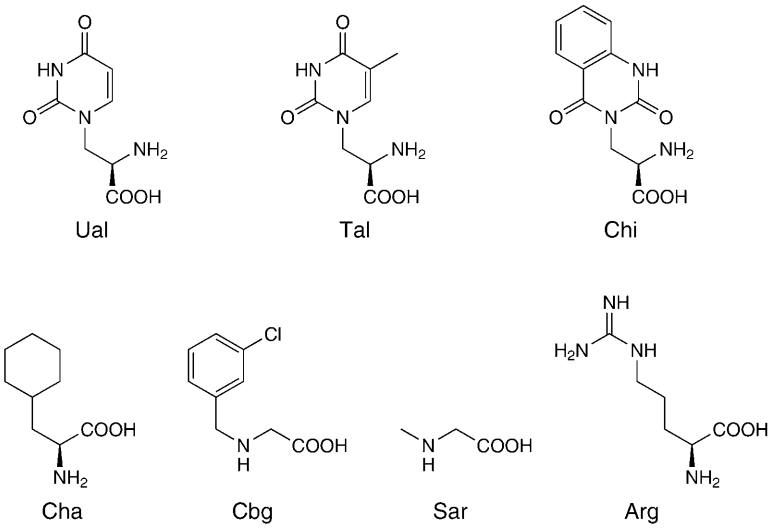

Fig 1. *Amino acid building blocks used for the synthesis of the oligopeptides Ac-Arg-Ual-Sar-Chi-Chi-Chi-Arg-NH_2 and Ac-Arg-Cbg-Cha-Chi-Chi-Tal-Arg-NH_2.* Ual = β-(Uracil-1-yl)-D-alanine, Tal = β-(thymin-1-yl)-D-alanine, Chi = β-(1,2,3,4-tertrahydro-2,4-dioxoquinazolin-3-yl)-D-alanine, Cha = β-(cyclohexyl)-L-alanine, Cbg = 2-[(3-(chlorobenzyl)amino]acetic acid, Sar = sarcosine, Arg = L-arginine.

We first started to optimize the Sar position, while the Ual position remained fixed. Eight new amino acids were selected. Since hydrophobic interactions seem to play a role in DNA recognition by short peptides [7], amino acids with hydrophobic side chain groups were selected (Ala, Leu). Alanine (Ala) was selected to investigate the potential difference with Sar, since their only difference lies in the different position of the side-chain Me group, *i.e.*, at the C(α)- and the N-atom, respectively. Furthermore, to increase the potential dipole interaction and H-binding capacities of the oligopeptides with dsDNA, also amino acids with polar groups were selected (Hse, Tyr, His, Thi, Phe($p$$NO_2$), and Phe($p$F); *cf. Fig. 2*).

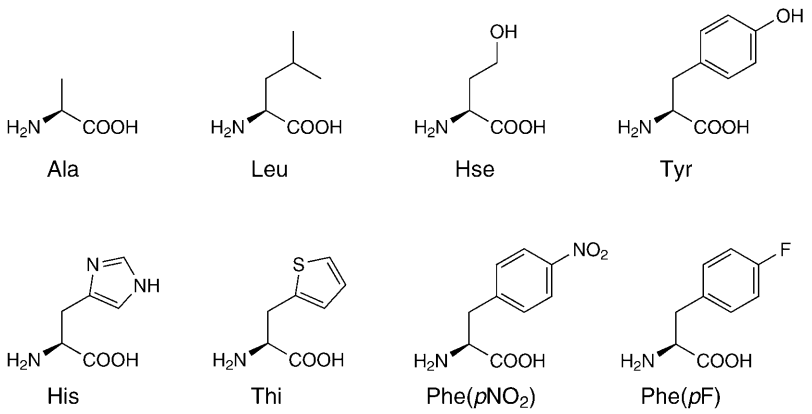

Fig. 2. *Structure of the newly introduced amino acids.* Ala = L-Alanine, Leu = L-leucine, Hse = L-homoserine, Tyr = L-tyrosine, His = L-histidine, Thi = L-thienylalanine, Phe(pNO$_2$) = p-nitro-L-phenylalanine, Phe(pF) = p-fluoro-L-phenylalanine.

The oligopeptides were synthesized on solid-support using the *Rink* amide MBHA resin[1]). Amino acid building blocks were coupled with activation mixtures consisting of 4 equiv. of amino acid (AA), 4 equiv. HOBt, 2 equiv. PyBOP, 4 equiv. DIC and 4 equiv. of EtN(i-Pr)$_2$ with respect to the solid-support. After deprotection and cleavage upon TFA treatment, the individual oligopeptides were purified by reversed-phase HPLC and analyzed by mass spectrometry.

All oligopeptides were tested against a 14-bp semi palindromic sequence (5′-AGATTGTGCAATGT-3′), which was also used during previous selection procedures. Binding affinities of the peptide ligands were determined using the high-throughput FID assay in a 96-well format as described by *Boger et al.* [8]. The test relies on the fluorescence decrease derived from the displacement of dsDNA-bound ethidium bromide (EtBr) by a DNA-binding ligand. It is established that EtBr does not inhibit the binding mode of the competitive ligand. The fluorescence decrease is directly related to the extent of DNA binding. In a 100-µl assay volume, 1 µM dsDNA (14 µM in base pairs (bp)) and 7 µM EtBr were used, establishing the optimal 1:2 EtBr/bp ratio. A 10 mM *Tris* + 10 mM NaCl buffer at pH 7.4 was used. Repeated measurements with different oligopeptide concentrations were performed to calculate average values. *Fig. 3* illustrates the influence of the different amino acid substitutions on the binding affinity of the oligopeptide with the different 14-bp dsDNA target.

Selective substitution of the Sar position turned out to be a feasible method to improve the dsDNA-binding affinity of the oligopeptides. However, differences were observed between the different amino acid side chains. Based on the amount of EtBr displaced, a rank order of the DNA-binding affinity could be established: Ala < Phe(pF) < His < **Sar (= Ref)** < Hse < Thi ≈ Leu < Tyr < Phe(pNO$_2$). Substitution of Sar by Ala, His or Phe(pF) decreased the binding affinity in comparison with the reference

[1]) For all abbreviations, see *Exper. Part.*

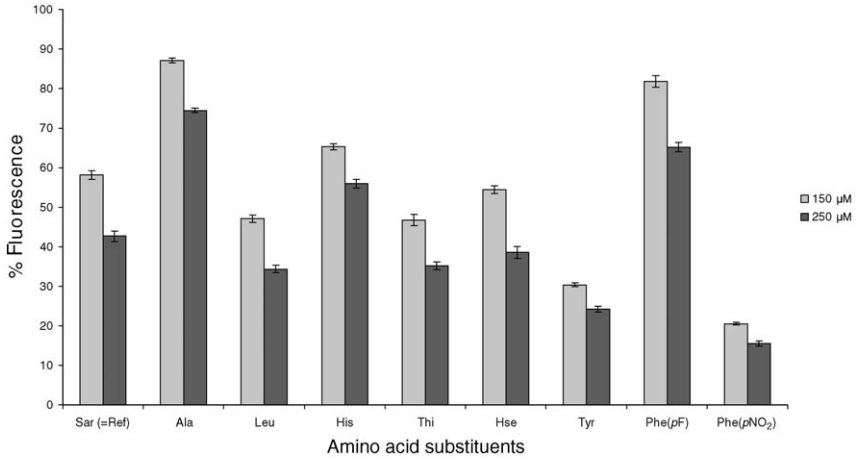

Fig. 3. *Fluorescent-intercalator-displacement assays for the oligopeptides substituted for the Sar position using the 14-mer dsDNA as target sequence.* The bar diagrams, representing the fluorescence decrease, give an indication of the binding affinity of the different oligopeptides in comparison with the reference oligopeptide Ac-Arg-Ual-Sar-Chi-Chi-Chi-Arg-NH_2 (=Ref). Binding affinities were measured at concentrations of 150 and 250 μM.

oligopeptide. The difference between Phe(*p*F) and Tyr is remarkable. Substitution of Sar by Tyr and Phe($p$$NO_2$) resulted in an improvement in dsDNA-binding affinity. Both amino acids contain an aromatic ring substituted with a polarizable group.

To quantify the increase in binding affinity upon substitution of Sar by Tyr or Phe($p$$NO_2$), apparent dissociation constants (K_d) were determined using the FID assay. Peptide concentrations were chosen in the range of 1 μM to 0.1 mM, using concentration increments of 2 μM final peptide concentration. The K_d value was determined as the peptide concentration at which the EtBr fluorescence intensity is decreased by 50%. The values obtained are averaged from three experiments. The results of these K_d determinations are collected in *Table 1*.

Table 1. *Dissociation Constants of the Selected Oligopeptides Containing an Amino Acid Substitution at the Sar Position*

Selected oligopeptide sequence	K_d[a]) [M]
Ac-Arg-Ual-Sar-Chi-Chi-Chi-Arg-NH_2 (=Ref)	20×10^{-5}
Ac-Arg-Ual-**Tyr-**Chi-Chi-Chi-Arg-NH_2	3.5×10^{-5}
Ac-Arg-Ual-**Phe(*p*NO_2)**-Chi-Chi-Chi-Arg-NH_2	2.8×10^{-5}

[a]) The K_d values are averaged from three measurements.

Substitution of Sar by Phe($p$$NO_2$) yielded a K_d value of 2.8×10^{-5} M. This is a sevenfold improvement of the binding affinity in comparison with the reference oligopeptide Ac-Arg-Ual-Sar-Chi-Chi-Chi-Arg-NH_2, which possessed a K_d value of 2.0×10^{-4} M.

Also substitution of Sar by Tyr resulted in a sixfold improvement of the binding affinity for the dsDNA target.

These results show that site-selective substitution of one amino acid by another can result in a considerable enhancement of the binding affinity. The peptide Ac-Arg-Ual-Phe(pNO$_2$)-Chi-Chi-Chi-Arg-NH$_2$ was selected for further optimization of the Ual position while the Phe(pNO$_2$) position remained fixed.

Three amino acids were selected for optimization of the Ual position. Tyrosine (Tyr) was again selected because of the good binding benefit upon substitution of Sar. Histidine (His) was selected based on the lexitropsin model [2][9]. Lysine (Lys) was introduced to investigate the effect of introduction of an additional positive charge into the peptide chain. These three oligopeptides were synthesized according to the same solid-phase peptide synthesis (SPPS) protocols as mentioned for the Sar substituents. The FID assay was also performed as described before. *Fig. 4* gives an overview of the influence of the different amino acid substitutions on the binding affinity of the oligopeptide with the 14-bp dsDNA target.

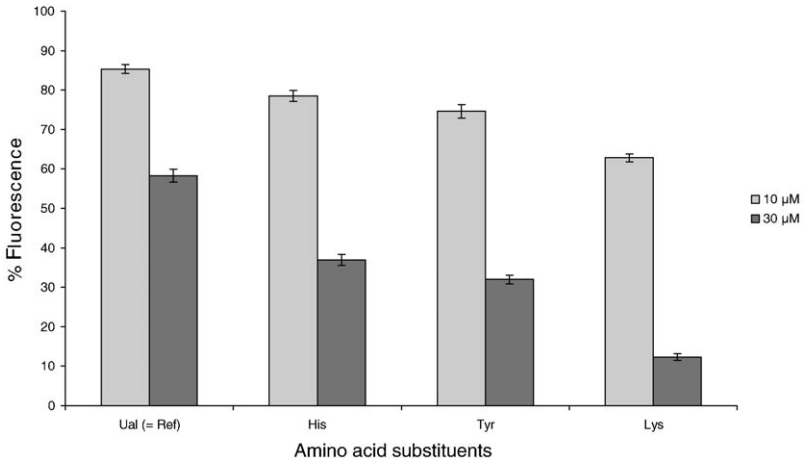

Fig. 4. *Fluorescent-intercalator-displacement assays for the oligopeptides substituted for the Ual position using the 14-mer dsDNA as target sequence.* The bar diagrams, representing the fluorescence decrease, give an indication of the binding affinity of the different oligopeptides in comparison with the reference oligopeptide Ac-Arg-Ual-Phe(pNO$_2$)-Chi-Chi-Chi-Arg-NH$_2$ (= Ref). Binding affinities were measured at concentrations of 10 and 30 μM.

Evaluation of the results of the FID assay reveals that we are able to further enhance slightly the binding affinity of the oligopeptide by selective substitution of the Ual position. An improvement of the binding affinity could be achieved with Lys.

Using the FID assay with 2-μM concentration increments of peptides within a range from 3 to 60 μM, apparent dissociation constants could be determined. The obtained values are averaged from three experiments. The results of these K_d determinations are shown in *Table 2*.

Substitution of Ual by His and Tyr did not give any significant improvement of the binding affinity in comparison with the reference oligopeptide Ac-Arg-Ual-

Table 2. *Dissociation Constants* K_d *of the Peptides Containing an Amino Acid Substitution at the Ual and Sar Positions*

Selected peptide sequences	K_d[a]) [M]
Ac-Arg-Ual-Sar-Chi-Chi-Chi-Arg-NH_2 (= Lead)	20×10^{-5}
Ac-Arg-Ual-Phe($p$$NO_2$)-Chi-Chi-Chi-Arg-$NH_2$ (= Ref)	2.8×10^{-5}
Ac-Arg-**His**-Phe($p$$NO_2$)-Chi-Chi-Chi-Arg-$NH_2$	2.7×10^{-5}
Ac-Arg-**Tyr**-Phe($p$$NO_2$)-Chi-Chi-Chi-Arg-$NH_2$	2.6×10^{-5}
Ac-Arg-**Lys**-Phe($p$$NO_2$)-Chi-Chi-Chi-Arg-$NH_2$	1.1×10^{-5}

[a]) The K_d values are averaged from three measurements.

Phe($p$$NO_2$)-Chi-Chi-Chi-Arg-$NH_2$. Introduction of an additional positive charge upon substitution of Ual by Lys resulted in a further 2.5-fold improvement of the binding affinity and a 20-fold improvement ($K_d = 1.1\times10^{-5}$ M) in comparison with the starting lead peptide Ac-Arg-Ual-Sar-Chi-Chi-Chi-Arg-NH_2.

The binding affinity of the oligopeptide Ac-Arg-Tyr-Phe($p$$NO_2$)-Chi-Chi-Chi-Arg-$NH_2$ is of the same order of magnitude as the binding affinity of the oligopeptide Ac-Arg-Cbg-Cha-Chi-Chi-Chi-Arg-NH_2 ($K_d = 3.5\times10^{-5}$ M), which was previously optimized for the Ual-Sar positions using other amino acid building blocks [7]. The variability that may be introduced in both positions points to aspecific interactions.

Synthesis of New dsDNA-Binding Hybrid Molecules. Several examples exist of DNA-binding natural products such as actinomycin D [10–12] and echinomycin [10], which use a bimodal cooperative intercalation/groove-binding mechanism for molecular recognition of DNA. In early design efforts towards artificial mimics of these natural products, combinations of intercalators such as acridine and phenoxazone, and groove binders derived from netropsin and distamycin A were synthesized [13–15]. Based on these models, we decided to introduce an intercalating unit into the peptide sequence in order to develop different types of oligopeptide–intercalator conjugates.

Acridine was, because of its synthetic accessibility, the most obvious choice as intercalator for the design of dsDNA-binding hybrid molecules.

Acridine-9-carboxylic acid was coupled with protected lysine to give (*2S*)-6-{[(acridin-9-yl)carbonyl]amino}-2-({[(9*H*-fluoren-9-yl)methoxy]carbonyl}amino)hexanoic acid (Lys(Acr)), which can be used in traditional peptide-synthesis protocols. In this way, the oligopeptide-intercalator chain can be further elongated from the N-terminal intercalator end, if needed. The lysine-derivatized intercalator Lys(Acr) was synthesized by coupling the ε-amino function of N^{α}-Fmoc-L-lysine to acridine-9-carboxylic acid using HATU as peptide coupling reagent (*Scheme 1*).

Oligopeptide–Acridine Conjugates (*PAC*). One of the best known examples of DNA binding by a combination of groove binding and intercalation is NetGA (*Fig. 5*) [13]. For this reason, NetGA was used as a model to construct new oligopeptide–acridine conjugates (PAC). The oligopeptide and intercalator were coupled using linker arms of different length and flexibility in order to allow collaborative binding of the two DNA-binding domains (*Fig. 5*). Using glycine (Gly) and β-alanine (β-Ala) combinations, spacer lengths of 3, 4, 6, and 7 atoms could be obtained. The more flexible linker, 4-aminobutanoic acid (GABA; 5-atoms length), was added because it offered

Scheme 1. *(2S)-6-{[(Acridin-9-yl)carbony])amino}-2-({[(9H-fluoren-9-yl)methoxy]carbonyl}amino)-hexanoic Acid* (**2**; Lys(Acr))

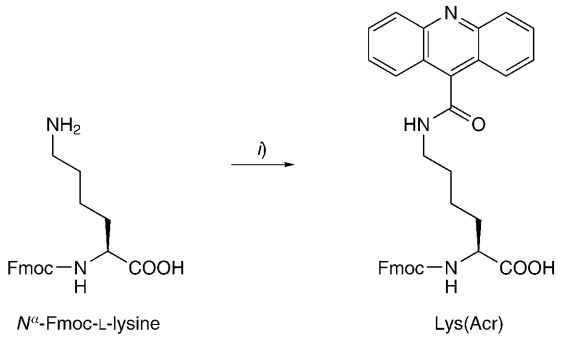

i) Acridine-9-carboxylic acid, HATU, DIEA, DMF.

the optimum fit for several known hybrid molecules. Finally, 6-Ahx (6-aminohexanoic acid) was selected to investigate the importance of the flexibility of the spacers. Three oligopeptides with different DNA-binding affinities were selected for coupling with the new intercalating unit:

Ac-Arg-Ual-Sar-Chi-Chi-Chi-Arg-NH_2 (**A**) $K_d = 20.0 \times 10^{-5}$ M

Ac-Arg-Cbg-Cha-Chi-Chi-Tal-Arg-NH_2 (**B**) $K_d = 3.5 \times 10^{-5}$ M

Ac-Arg-Lys-Phe($p$$NO_2$)-Chi-Chi-Chi-Arg-$NH_2$ (**C**) $K_d = 1.1 \times 10^{-5}$ M

Synthesis of the PACs was performed on the *Rink* amide MBHA resin by using standard coupling reagents for peptide-bond formation and Fmoc-protected amino acids. The amino acid (AA) building blocks were coupled using activation mixtures consisting of 4 equiv. of AA, 4 equiv. of HOBt, 2 equiv. of PyBOP, 4 equiv. of DIC, and 4 equiv. of $EtN(i\text{-}Pr)_2$ with respect to the solid support. Incorporation of the new synthesized intercalating unit into the oligopeptide sequence was also performed under the same reaction conditions. The crude material obtained after TFA cleavage was purified by reversed-phase HPLC and analyzed by mass spectrometry.

Acridine shows no fluorescence under the test conditions and also no quenching of the EtBr fluorescence signal. These results show that the FID assay is suitable for determination of the binding affinity of different types of oligopeptide–acridine conjugates. The experiments were performed with the original 14-bp dsDNA sequence as target. After incubation of the DNA/EtBr/ligand mixture at room temperature for 30 min, each well was read on a fluorescent plate reader (*Fig. 6*).

The FID measurements with the PACs derived from lead **A** reveal that incorporation of an intercalating unit with any linker arm leads indeed to higher dsDNA-binding affinities in comparison with the unconjugated reference oligopeptides. However, little differences are observed between the different linker molecules. With the coupling of acridine-9-carboxylic acid to lysine, already a flexible C_4 linker was introduced between the oligopeptide chain and the intercalating core, apparently decreasing the importance

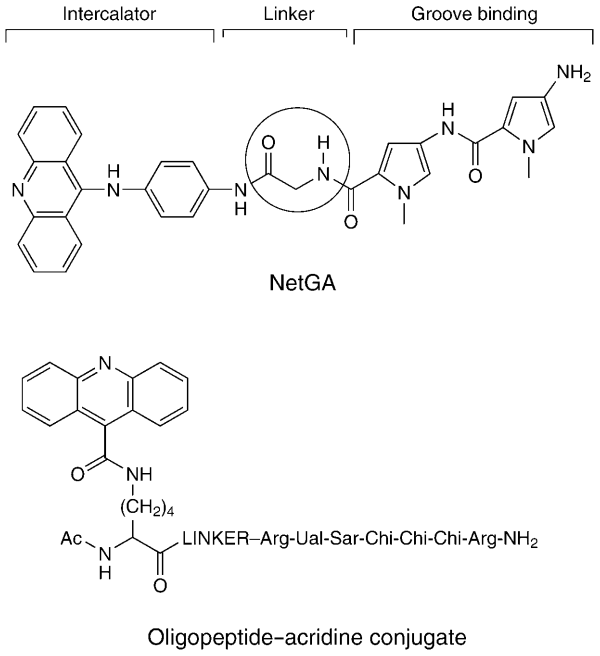

Fig. 5. *Structural comparison between NetGA and the PAC library.* The different building blocks are presented together with their relevance for dsDNA binding.

of the presence of an additional linker arm. For this reason, less linker molecules were selected for the synthesis of the two other PAC series.

Also for the two other PAC series, we can conclude that there is a binding benefit upon coupling of an intercalating unit. In general, little differences are observed between the different linker molecules. For the seven-atom linker arms (Gly-β-Ala and 6-Ahx), there is a slight preference for the more flexible 6-Ahx linker in comparison with the Gly-β-Ala linker. This preference for relatively long and more flexible linker arms is in accordance with known described hybrid molecules.

To quantify the positive effect of coupling an intercalating unit on the DNA-binding affinity, apparent dissociation constants (K_d) of the conjugates were determined. As a reference, also the binding affinity of acridine-9-carboxylic acid for the 14-bp dsDNA target was determined. The results of the K_d determinations are shown in *Table 3*.

The K_d values confirm the positive effect upon coupling of a peptide sequence to the acridine unit and *vice versa*. Nevertheless, acridine does not give the same binding benefit to all three reference oligopeptides. Conjugation to acridine gives an eightfold improvement of the binding affinity for lead **A**, only a twofold improvement for lead **B**, and only a very slight improvement for lead **C** (based on the K_d values of the conjugates with the highest binding affinity). After introduction of acridine, all conjugates have a binding affinity ranging from 1 to 3×10^{-5} M for the 14-bp dsDNA target.

Design and Synthesis of Peptide–Bisacridine Conjugates (PbAC). Coupling of the newly synthesized intercalating moiety has a positive but limited effect on the binding

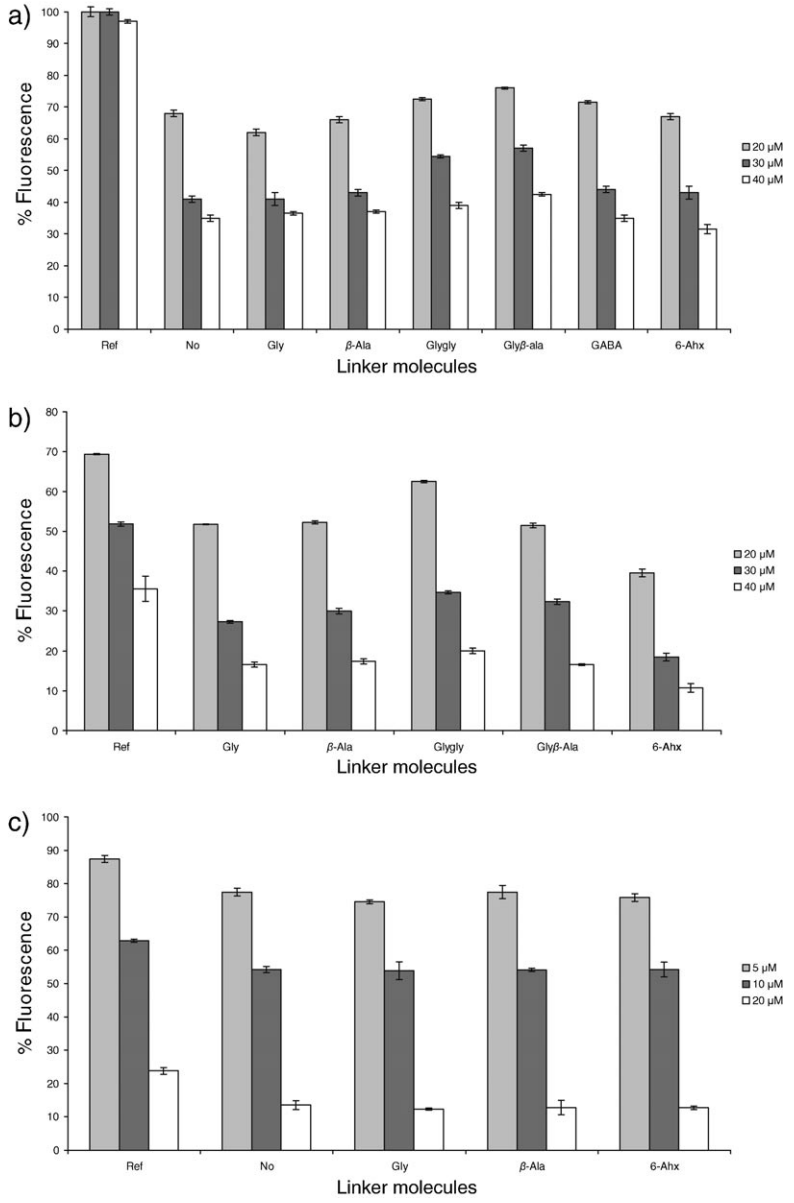

Fig. 6. *Fluorescent-intercalator-displacement assays for the different PACs with the 14-bp dsDNA sequence as target.* The bar diagrams, representing the fluorescence decrease, give an indication of the binding affinity of the different PACs in comparison with their reference oligopeptide Ac-Arg-Ual-Sar-Chi-Chi-Chi-Arg-NH_2 (**A**) (*a*), Ac-Arg-Cbg-Cha-Chi-Chi-Tal-Arg-NH_2 (**B**) (*b*), and Ac-Arg-Lys-Phe(*p*NO_2)-Chi-Chi-Chi-Arg-NH_2 (**C**) (*c*).

Table 3. K_d *Values of the Selected PACs in Comparison with Their Parent Oligopeptides*

Oligopeptide–acridine sequences	K_d[a]) [M]
Derived from lead **A**:	
Acridine-9-carboxylic acid	100×10^{-5}
Ac-Arg-Ual-Sar-Chi-Chi-Chi-Arg-NH_2 (=Ref)	20×10^{-5}
Ac-**Lys(acr)**-Arg-Ual-Sar-Chi-Chi-Chi-Arg-NH_2	3.0×10^{-5}
Ac-**Lys(acr)-Gly**-Arg-Ual-Sar-Chi-Chi-Chi-Arg-NH_2	2.8×10^{-5}
Ac-**Lys(acr)-β-Ala**-Arg-Ual-Sar-Chi-Chi-Chi-Arg-NH_2	2.9×10^{-5}
Ac-**Lys(acr)-GABA**-Arg-Ual-Sar-Chi-Chi-Chi-Arg-NH_2	3.0×10^{-5}
Ac-**Lys(acr)-6-Ahx**-Arg-Ual-Sar-Chi-Chi-Chi-Arg-NH_2	2.7×10^{-5}
Derived from lead **B**:	
Ac-Arg-Cbg-Cha-Chi-Chi-Tal-NH_2 (=Ref)	3.5×10^{-5}
Ac-**Lys(Acr)-Gly-**Arg-Cbg-Cha-Chi-Chi-Tal-NH_2	2.0×10^{-5}
Ac-**Lys(Acr)-β-Ala-**Arg-Cbg-Cha-Chi-Chi-Tal-NH_2	2.3×10^{-5}
Ac-**Lys(Acr)-Gly-Gly**-Arg-Cbg-Cha-Chi-Chi-Tal-NH_2	2.3×10^{-5}
Ac-**Lys(Acr)-β-Ala-Gly**-Arg-Cbg-Cha-Chi-Chi-Tal-NH_2	2.4×10^{-5}
Ac-**Lys(Acr)-6-Ahx**-Arg-Cbg-Cha-Chi-Chi-Tal-NH_2	1.9×10^{-5}
Derived from lead **C**:	
Ac-Arg-Lys-Phe(*p*NO_2)-Chi-Chi-Chi-Arg-NH_2 (=Ref)	1.1×10^{-5}
Ac-**Lys(Acr)-6-Ahx**-Arg-Lys-Phe(*p*NO_2)-Chi-Chi-Chi-Arg-NH_2	1.0×10^{-5}

[a]) The K_d values are averaged from three measurements.

affinity of lead peptides **A**, **B**, and **C**. These findings are in agreement with earlier results where direct coupling of acridine-9-carboxylic acid to the oligopeptide reinforced the DNA-binding strength in comparison with the unconjugated oligopeptides [16]. Therefore, we initiated the synthesis of oligopeptide–bisintercalator conjugates (PbAC) analogue to the quinoxaline antibiotics binding model. These antibiotics contain two intercalator entities connected by a cyclic depsipeptide serving as a constrained sequence-selective linker [10] (*Fig. 7*).

The PbACs are interesting to evaluate whether introduction of a second acridine unit can further enhance the dsDNA-binding affinity. The first intercalating moiety was introduced using linker arms of different length and flexibility in order to allow independent binding of the three DNA-binding domains (direct coupling, Gly, β-Ala, Glygly, Gly-β-Ala, GABA, 6-Ahx). The second acridine-9-carboxylic acid intercalating moiety was coupled to the oligopeptide sequence using a glycine linker selected from literature [16].

Using the *Rink* amide MBHA resin and the Lys(Acr) intercalator, the synthesis of the PbACs conjugates was straightforward as depicted in *Scheme 2*.

After functionalization of the resin with the Lys(Acr) intercalating moiety using 4 equiv. of Lys(Acr), 4 equiv. of HOBt, 2 equiv. of Pybop, 4 equiv. of DIC, and 4 equiv. of $EtN(i\text{-}Pr)_2$, a linker molecule was coupled, followed by further elongation of the peptide sequence using classical reagents for peptide coupling and Fmoc amino acids as described before. Final coupling of acridine-9-carboxylic acid was performed with HATU as described in [16]. After simultaneous deprotection and cleavage from the solid support upon TFA treatment, the crude peptide mixtures were purified by reversed-phase HPLC. The HPLC profiles of all PbACs showed one major peak of

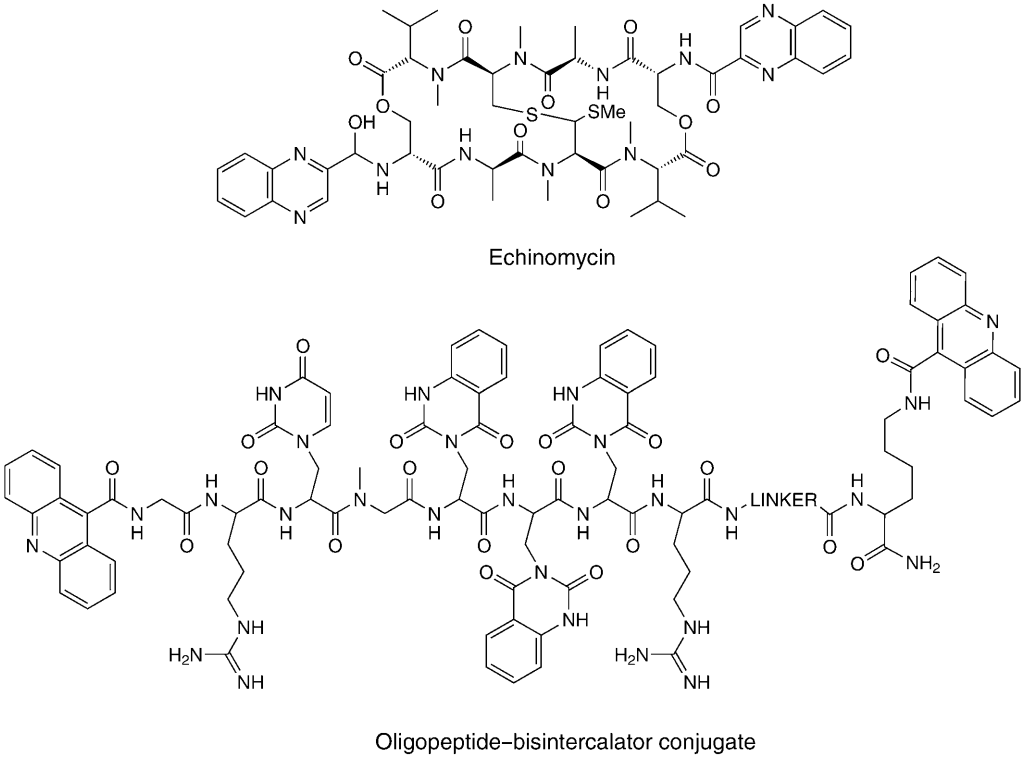

Fig. 7. *Structural similarity between echinomycin and the oligopeptide–bisintercalator conjugate library*

which the mass corresponded to the calculated mass of the desired compound. A more-polar side peak was always present, corresponding to the mono-acridine complex.

Binding affinities of the synthesized PbACs were investigated using the FID assay as described before. The results as depicted in *Fig. 8* reveal that there is only a very small binding benefit upon coupling of a second acridine unit. A slight preference may be observed using longer linker arms, although the effect is not really significant.

Apparent dissociation constants were determined, using the FID assay with ligand concentration increments of 1 μM, ranging from 10 to 50 μM final PbAC concentration. The results of the K_d determinations are shown in *Table 4*. These K_d values establish the limited binding benefit upon introduction of a second acridine unit.

Dipeptide–Acridine Conjugates (*DAC*). Facing the problem of the limited binding benefit upon coupling of an additional acridine unit to the PACs, we developed another series of hybrid molecules displaying a groove-binding/intercalation/groove-binding mechanism instead of an intercalation/groove-binding/intercalation binding mechanism. For the design of these dipeptide–acridine conjugates (DACs), actinomycin D was used as a model compound. Actinomycin D is a naturally occurring cytostatic agent, consisting of three main building blocks: a central planar 2-aminophenoxazine chromophore, flanked by two identical cyclic pentapeptide lactones [10–12] (*Fig. 9,a*). Using actinomycin D as a model compound, we designed series of DACs, consist-

Scheme 2. *Schematic Overview of the Solid-Phase Peptide Synthesis of Oligopeptide–Bisacridine Conjugates*

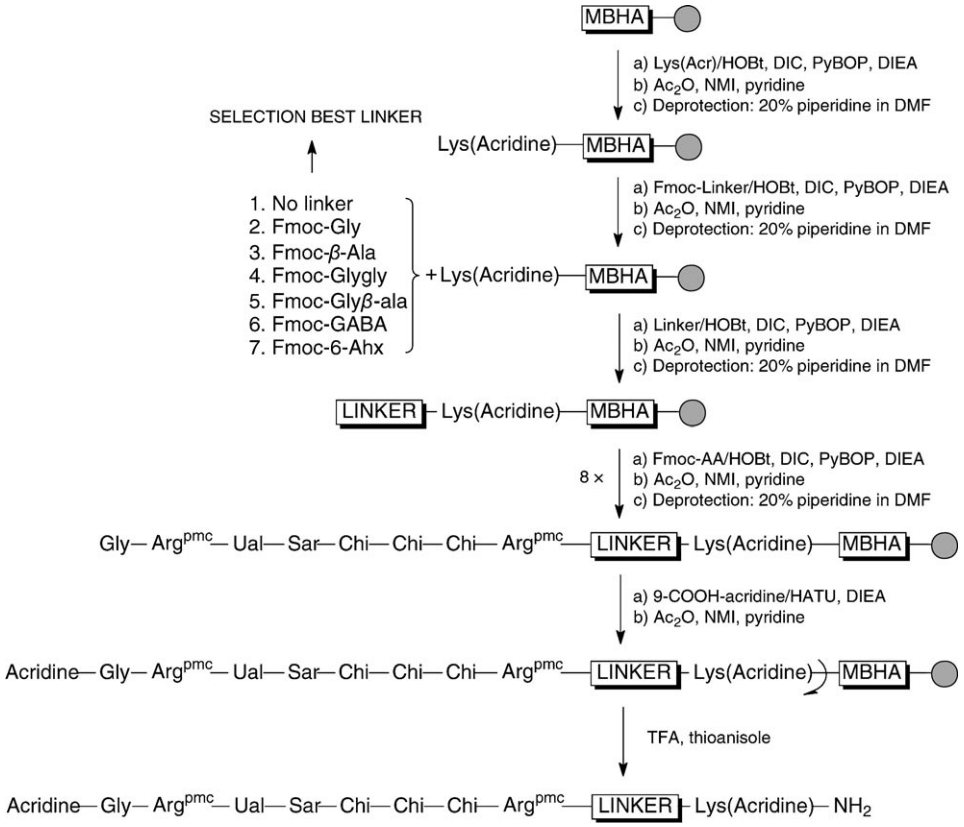

Table 4. K_d *Values of the PAC and Its Derived PbACs*

Oligopeptide–bisacridine conjugates	K_d[a]) [M]
Acr-Gly-Arg-Ual-Sar-Chi-Chi-Chi-Arg-NH_2	2.7×10^{-5}
Acr-Gly-Arg-Ual-Sar-Chi-Chi-Chi-Arg-***β*-Ala-Gly-Lys(Acr)**-NH_2	2.0×10^{-5}
Acr-Gly-Arg-Ual-Sar-Chi-Chi-Chi-Arg-**GABA-Lys(Acr)**-NH_2	1.7×10^{-5}
Acr-Gly-Arg-Ual-Sar-Chi-Chi-Chi-Arg-**6-Ahx-Lys(Acr)**-NH_2	1.7×10^{-5}

[a]) The K_d values are averaged from three measurements.

ing of a central acridine intercalating moiety, flanked by two oligopeptides (*Fig. 9, b*). Both oligopeptides were coupled to the intercalating moiety with linker arms of different length and flexibility in order to allow independent binding of all three DNA-binding domains. The first linker was already selected out of the series of PACs where 6-Ahx turned out to be the best linker arm.

Two oligopeptides with different binding affinities were selected as leads for the synthesis of the DACs:

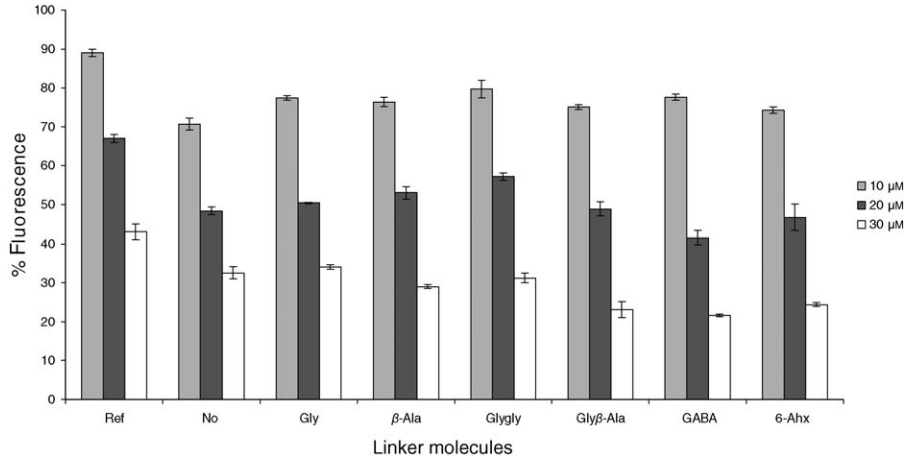

Fig. 8. *Fluorescent intercalator displacement assays for the different PbACs derived from Acr-Gly-Arg-Ual-Sar-Chi-Chi-Chi-Arg-NH_2 with the 14-bp dsDNA sequence as target.* The bar diagrams, representing the fluorescence decrease, give an indication of the binding affinity of the different PbACs in comparison with the reference oligopeptide Acr-Gly-Arg-Ual-Sar-Chi-Chi-Chi-Arg-NH_2 (=Ref). Binding affinities were measured at concentrations of 10, 20, and 30 μM.

Ac-Arg-Ual-Sar-Chi-Chi-Chi-Arg-NH_2 (**A**) $K_d = 20.0 \times 10^{-5}$ M

Ac-Arg-Cbg-Cha-Chi-Chi-Tal-Arg-NH_2 (**B**) $K_d = 3.5 \times 10^{-5}$ M

Using these lead peptides, three series of DACs were designed. The conjugates were synthesized in such a way that we end up with partially or fully symmetrical compounds as shown in *Scheme 3*.

Synthesis of these DACs by simple elongation of the peptide sequence from the intercalating unit Lys(Acr) implies that the second oligopeptide sequence had to be synthesized in opposite direction in comparison with the usual synthesis direction. To investigate the coupling yields, when synthesis was achieved in a reversed direction, two test peptides, Ac-Arg-Chi-Chi-Chi-Sar-Ual-Arg-NH_2 and Ac-Arg-Tal-Chi-Chi-Cha-Cbg-Arg-NH_2, were synthesized on solid-support using the same reaction conditions as for the usual oligopeptides. To investigate coupling efficiencies, fulvene-piperidine determinations or *Kaiser* tests were performed after each amino acid introduction. The amino acids Cha, Cbg, and the second Arg (Arg2) had to be coupled twice in order to obtain at least 95% yield. After cleavage from the solid-support upon TFA treatment, the peptides were purified by reversed-phase HPLC and analyzed by mass spectrometry. The chromatogram showed in both cases one major peak (>85%), corresponding to the mass of the desired peptide sequence. A minor side peak was present which was not further investigated due to its presence in low concentration. The DACs were synthesized on the *Rink* amide MBHA resin by further elongation of the PAC sequence from the intercalator according to *Scheme 3*. The AA building blocks were coupled using activation mixtures consisting of 4 equiv. of AA, 4 equiv. of HOBt, 2 equiv. of PyBOP, 4 equiv. of DIC, and 4 equiv. of EtN(i-Pr)$_2$ with

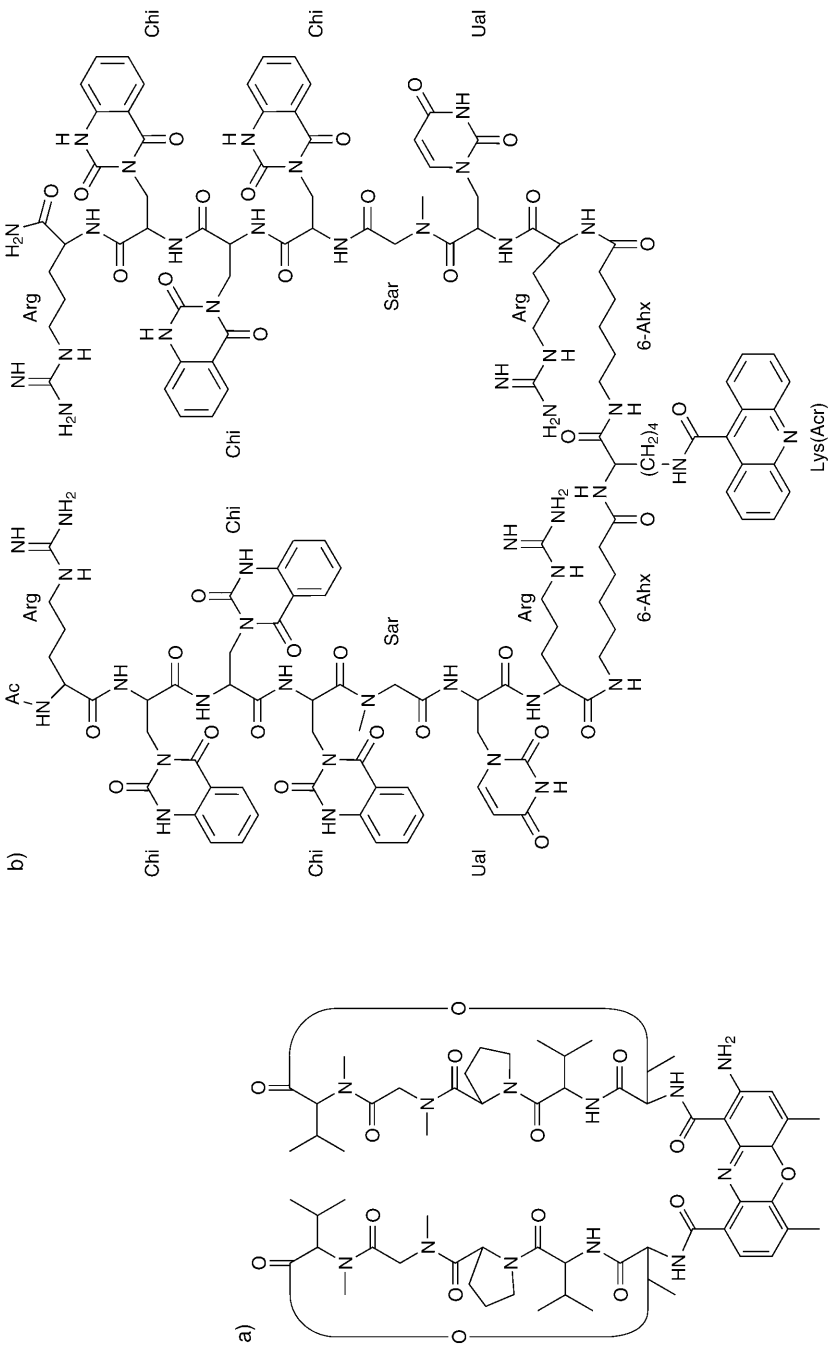

Fig. 9. *Structural similarity between actinomycin D and dipeptide–acridine conjugate Ac-Arg-Chi-Chi-Chi-Sar-Ual-Arg-6-Ahx-Lys(Acr)-6-Ahx-Arg-Ual-Sar-Chi-Chi-Chi-Arg-NH*$_2$

Scheme 3. *Schematic Overview of the Solid-Phase Peptide Synthesis of Dipeptide–Acridine Conjugates Derived from Lead A*

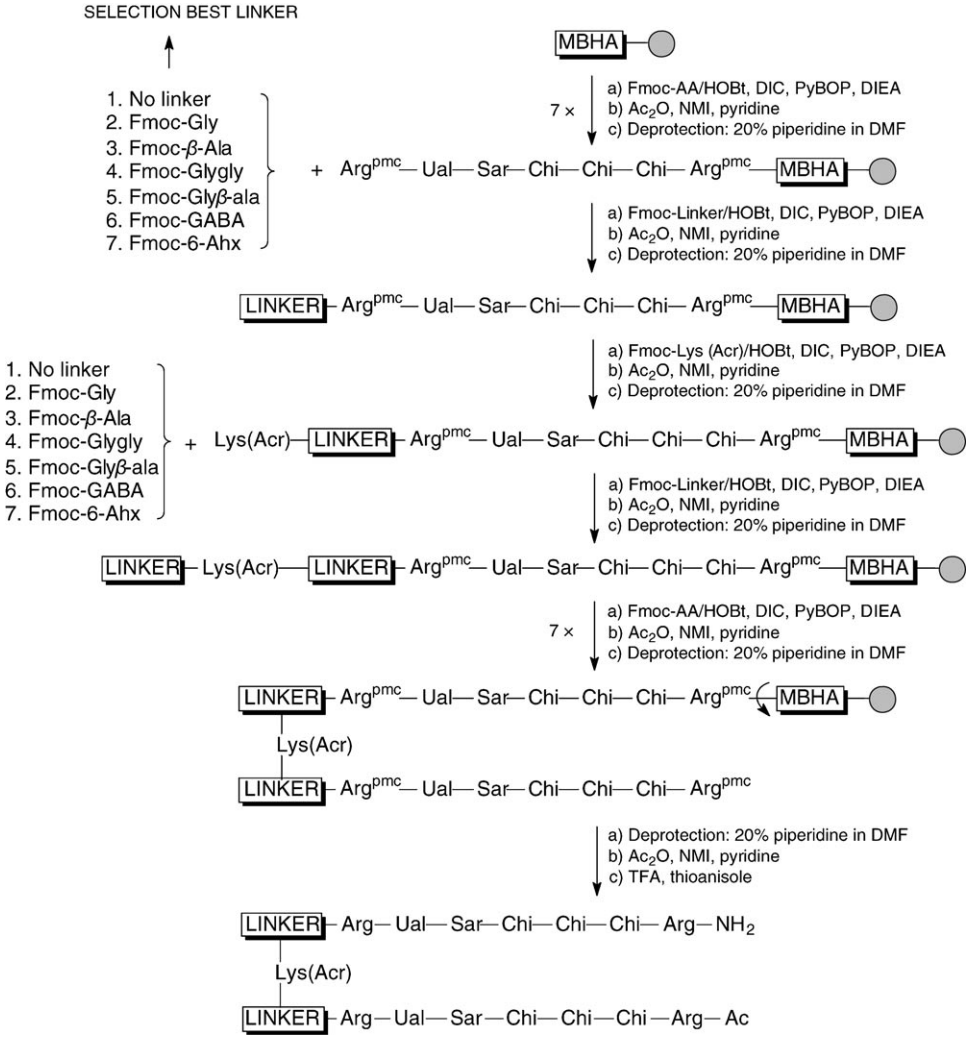

respect to the solid-support. Cbg, Cha, and Arg2 of the second peptide sequence were coupled twice. The mixtures obtained after cleavage upon TFA treatment were purified by reversed-phase HPLC. The HPLC profile showed one major peak, of which the mass corresponded to the calculated mass of the desired conjugate, together with two or three contaminant peaks in low yields, corresponding to incomplete amino acid couplings.

Characterization of the DACs was performed by tandem mass spectrometry to verify the sequence of the synthesized DACs containing unnatural amino acids. Sequencing peptides is based on assigning the fragment ions obtained by collision-induced dis-

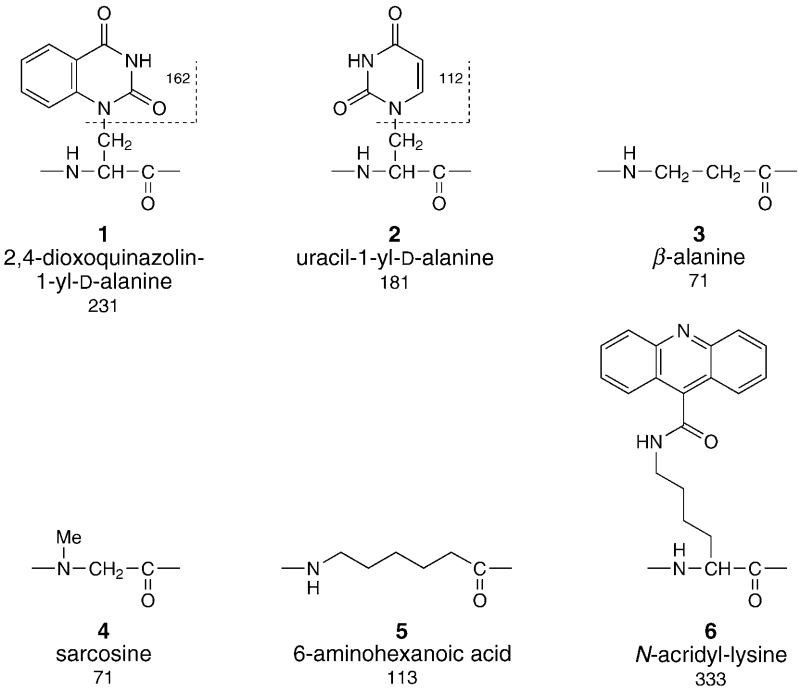

Fig. 10. *Structures and residue masses of the amino acids incorporated in the dipeptide–acridine conjugates*

sociation (CID). For peptides consisting of natural amino acids, this has become fairly easy and reliable thanks to the software programs currently available. The assignment of all fragmentation peaks derived from peptides consisting of natural amino acids is based on a standard nomenclature proposed by *Roepstorff* and *Fohlman* [17], where the N-terminal ions are represented by the symbols a_n, b_n, and c_n, and the corresponding C-terminal ions are represented by x_n, y_n, and z_n. However, sequencing peptides containing modified amino acids is not straightforward when the peptides do not follow the fragmentation rules of natural amino acid containing peptides. Here, the fragmentation of dipeptide–intercalator conjugates containing the amino acid moieties shown in *Fig. 10* is studied in order to be able to sequence these peptides *de novo*.

The different DACs derived from lead **A** were transformed to their coded sequences as depicted in *Table 5*.

As an example, the spectra obtained for peptide I are shown. The fragmentation spectrum obtained by CID of the doubly charged $[M+2\,H]^{2+}$ precursor ion (*m/z* 1547) shows peaks at *m/z* 1490.9, 1465.7, 1410.0, and 1384.8 that can be assigned to the loss of 112 (uracil side chain from **2**), 162 (quinazoline dione from **1**), 112+162, and 162+162, respectively (*Fig. 11*). The ion at *m/z* 980.3 corresponds to the amide cleavage product at the uracil containing amino acid (corresponding to the c″ ion).

Upon fragmentation of this ion, consecutive losses of 162 and 88 agree with the loss of the side chain from **1** and the loss of sarcosine amide, respectively. Loss of 231 cor-

Table 5. *Coded Sequences of Peptides Containing Synthetic Amino Acids.* Numbers refer to structures in *Fig. 10*, letters to regular amino acid codes.

No.	Coded sequence	M_r
I	AcNH-R11142R365R24111R-$CONH_2$	3093
II	AcNH-R11142RGG65R24111R-$CONH_2$	3134
III	AcNH-R11142R3G65R24111R-$CONH_2$	3148
IV	AcNH-R11142R565R24111R-$CONH_2$	3133
V	AcNH-R11142RG65R24111R-$CONH_2$	3079
VI	AcNH-65R24111R-$CONH_2$	1762

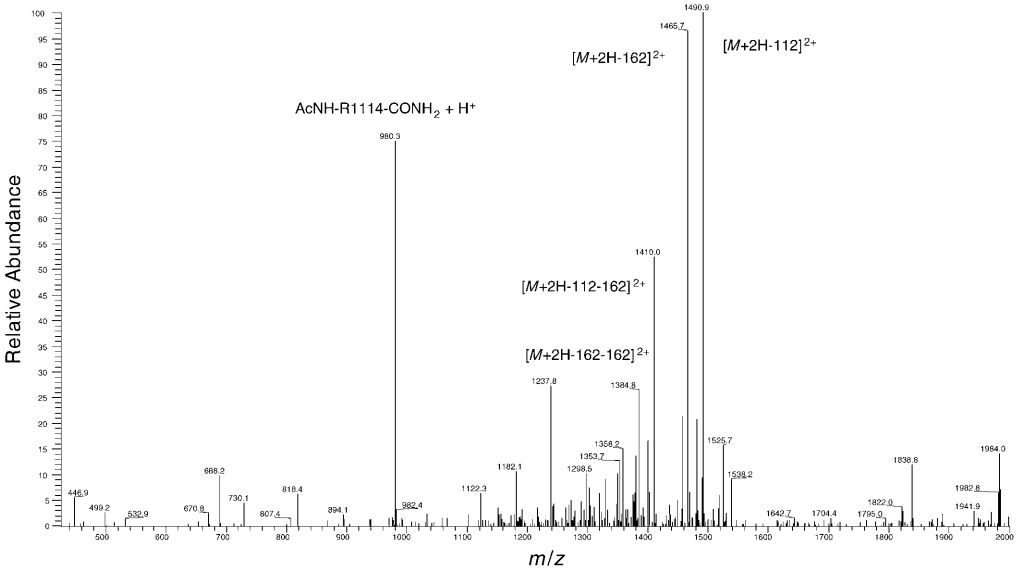

Fig. 11. *Fragment-ion spectrum for peptide I.* Daughter ion analysis of *m/z* 1547.

responds to the cleavage of a dioxoquinazolinyl amino acid **1** (*Fig. 12*). After loosing *m/z* 980, the remaining part yields *m/z* 1984 (*Fig. 11*). This ion also lacks the uracil group and NH_3. Further fragmentation of this ion (MS/MS/MS) confirms the sequence. Because of the easy loss of NH_3, the 'wideband activation' option was used during acquisition. It will cause fragmentation, not only for the selected precursor ion, but also for the $[M+H-NH_3]^+$ ion.

Additional information can be obtained by in-source fragmentation. Because of the 30% cut-off property of ion traps, fragments of low *m/z* cannot be detected from high mass precursors. In-source fragmentation solves this problem if the sample is pure. The main peak at *m/z* 204 in *Fig. 13* is the acridinyl moiety.

Sequencing of these synthetic DACs was not directly possible from MS/MS because the fragmentation is complicated by the loss of side chains. MS^3 Experiments, however, allow further partial sequence determination that can be used to obtain at least parts of the sequence. The assignments are summarized in *Fig. 14*. Some of the fragments could not yet conclusively be assigned.

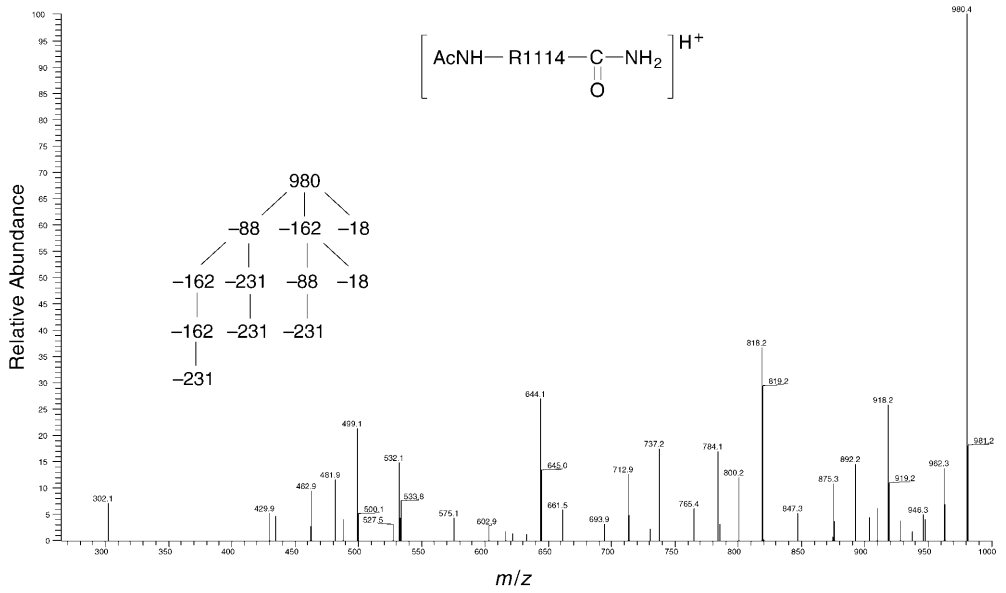

Fig. 12. *MS/MS/MS Spectrum of fragment* m/z *980 of peptide I*

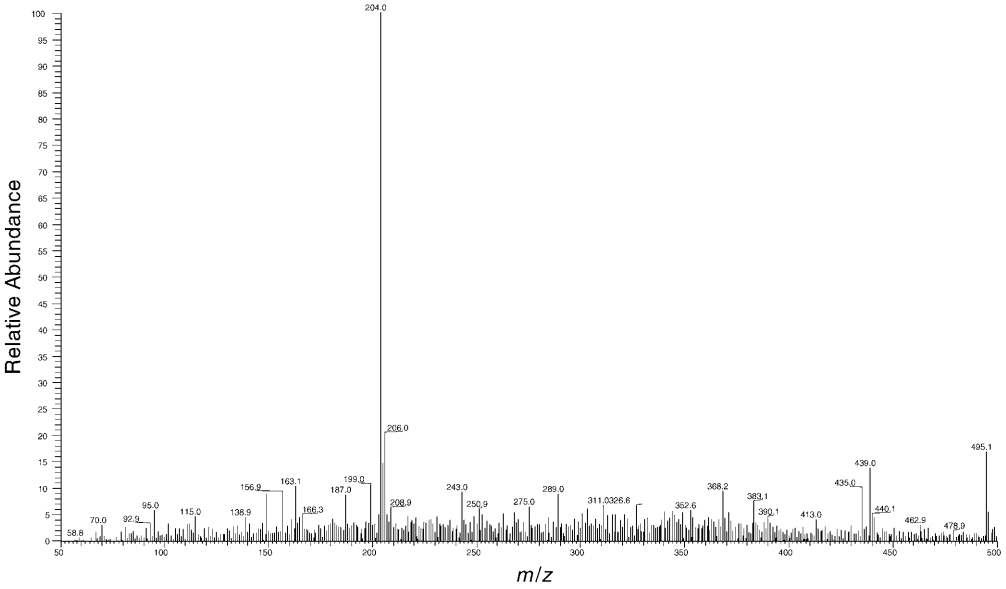

Fig. 13. *Spectrum obtained by in-source fragmentation of peptide I*

Binding affinities of the synthesized DACs were investigated using the FID assay as described before.

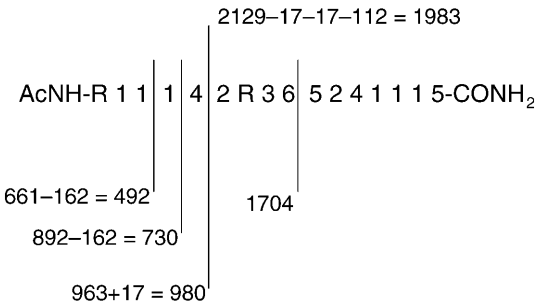

Fig. 14. *Assignment of fragment ions from* Fig. 12. Numbers in the sequence refer to structures in *Fig. 10.*

The results depicted in *Fig. 15* show that all DACs exhibit higher dsDNA-binding affinities in comparison with their parent PACs, since all experiments could be performed at lower concentrations. It has to be noted that, for the combi series, only one DAC was synthesized using a Gly linker arm. Also little differences are observed between the different linker molecules.

To obtain a more detailed rank order of the binding affinities of the different DACs in relation to each other and their parent PACs, apparent dissociation constants were determined using the FID assay with ligand concentration increments of 1 μM, ranging from 0.5 to 20 μM. To compare and to situate the DNA-binding affinities of the DACs within the group of known DNA-binding ligands, the DNA-binding affinity of *Hoechst 33258* was determined for one of its target sequences (5′-AAAAA-3′) using the FID assay. *Hoechst 33258* concentrations were chosen ranging from 0.1 to 3 μM, with concentration increments of 0.1 μM final *Hoechst 33258* concentration.

The target sequence was synthesized within a hairpin oligonucleotide (5′-GC**AAAAA**GAAAAAC**TTTTT**GC-3′). The results of the K_d determinations are collected in *Table 6*.

Table 6. K_d *Values of the Selected DACs in Comparison with Their Parent PACs*

Dipeptide–acridine sequences		K_d[a]) [M]
Derived from lead **1a**:		
	Hoechst 33258	0.1×10^{-5}
1a	-Lys(acr)-6-Ahx-Arg-Ual-Sar-Chi-Chi-Chi-Arg-NH_2 (=Ref)	2.7×10^{-5}
1b	Ac-Arg-Chi-Chi-Chi-Sar-Ual-Arg-**Gly**-Ref	1.1×10^{-5}
1c	Ac-Arg-Chi-Chi-Chi-Sar-Ual-Arg-***β*-Ala-Gly-**Ref	1.1×10^{-5}
1d	Ac-Arg-Chi-Chi-Chi-Sar-Ual-Arg-**6-Ahx**-Ref	1.0×10^{-5}
1e	Ac-Arg-Tal-Chi-Chi-Cha-Cbg-Arg-**Gly**-Ref (=combi)	$\mathbf{0.76\times10^{-5}}$
Derived from lead **2a**:		
2a	-Lys(acr)-6-Ahx-Arg-Cbg-Cha-Chi-Chi-Tal-Arg-NH_2 (=Ref)	1.9×10^{-5}
2b	Ac-Arg-Tal-Chi-Chi-Cbg-Cha-Arg-**Gly-Gly**-Ref	$\mathbf{0.82\times10^{-5}}$
2c	Ac-Arg-Tal-Chi-Chi-Cbg-Cha-Arg-**6-Ahx**-Ref	$\mathbf{0.74\times10^{-5}}$
2d	Ac-Arg-Tal-Chi-Chi-Cbg-Cha-Arg-**GABA**-Ref	$\mathbf{0.64\times10^{-5}}$

[a]) The K_d values are averaged from three measurements.

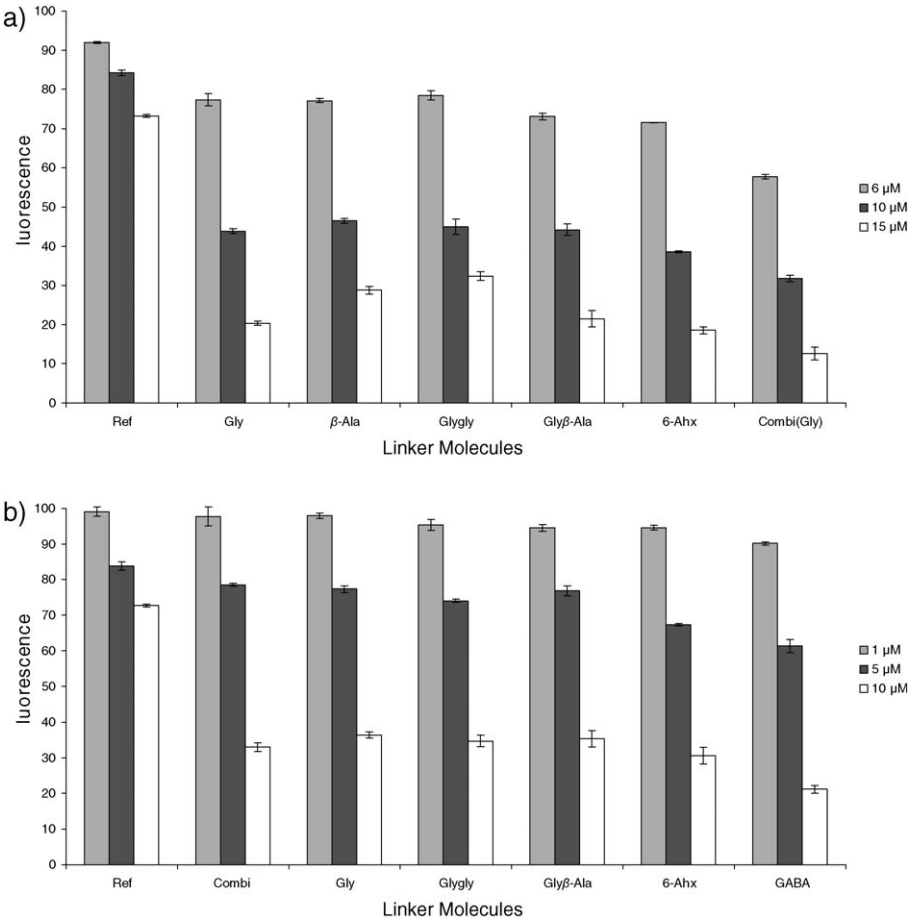

Fig. 15. *Fluorescent intercalator displacement assays for the different dipeptide–acridine conjugates built up from* a) *lead* **A** (Ac-Arg-Ual-Sar-Chi-Chi-Chi-Arg-NH_2) *and* b) *lead* **B** (Ac-Arg-Cbg-Cha-Chi-Chi-Tal-Arg-NH_2) *with the 14-bp dsDNA sequence as target*. The bar diagrams, representing the fluorescence decrease, give an indication of the binding affinity of the different dipeptide–acridine conjugates in comparison with their reference (= Ref) PAC *a*) Ac-Lys(Acr)-6-Ahx-Arg-Ual-Sar-Chi-Chi-Chi-Arg-NH_2 (**1a**) and *b*) Ac-Lys(Acr)-6-Ahx-Arg-Cbg-Cha-Chi-Chi-Tal-Arg-NH_2 (**2a**). The combi sequence, **1e**, represents Ac-Arg-Tal-Chi-Chi-Cha-Cbg-Arg-Gly-Lys(Acr)-6-Ahx-Arg-Cbg-Cha-Chi-Chi-Ta-Arg-NH_2. The linker molecules used to couple the second oligopeptide sequence to the intercalating unit are represented in the *x*-axis. Used DAC concentrations are indicated in the *Figure*.

The K_d values confirm that elongation of the peptide sequence from the acridine end could enhance the binding affinity for the 14-bp dsDNA-target sequence. For the DAC series derived from lead **1a**, a 2.5-fold improvement of the binding affinity could be obtained with the 6-Ahx linker, resulting in a binding affinity of 1.0×10^{-5} M for **1d**. The DAC combi sequence, **1e**, combining lead **A** and **B**, showed a 3.5-fold improvement of the binding affinity in comparison with the binding affinity of compound **1a**. Using this combination, a binding affinity in the low micromolar range up

to 7.6×10^{-6} M could be reached. Further enhancement of the binding affinity was achieved by dimerization of lead **B**. DAC **2d** is the most active compound from this series with a binding affinity of 6.4×10^{-6} M, which is a threefold improvement of the binding affinity in comparison with its parent PAC **2a** and in the same range as the binding affinity of the known minor-groove binder *Hoechst 33258* for its 5′-AAAAA-3′ target sequence having a K_d value of 1.0×10^{-6} M. This modified peptide is the strongest DNA binder of our series so far. If we compare this binding affinity with the binding strength of lead peptide **A** with value of a K_d of 2.0×10^{-4} M for the 14-bp dsDNA target, we can conclude that the binding affinity for the 14-bp dsDNA target is ultimately enhanced with a factor 30. However, since the $K_d^{conjugate} > (K_d^{peptide\ 1})\times(K_d^{peptide\ 2})$, we have to conclude that there is no positive cooperative association upon combination of the individual DNA-binding peptides into a single construct.

Conclusions. – In our effort to optimize the dsDNA-binding affinity of the lead peptides Ac-Arg-Ual-Sar-Chi-Chi-Chi-Arg-NH_2 (**A**) and Ac-Arg-Cbg-Cha-Chi-Chi-Tal-Arg-NH_2 (**B**), different strategies were evaluated. Investigations of glycine-substituted oligopeptide analogues revealed that the Ual and Sar positions were less important for interaction with the dsDNA target than the quinazoline dione (Chi) side chains. Therefore, one approach was focussed on the substitution of the Ual-Sar sequence within the oligopeptide Ac-Arg-Ual-Sar-Chi-Chi-Chi-Arg-NH_2 (**A**), with new amino acid side chains. Replacing the Ual-Sar sequence with new amino acid building blocks resulted in a eightfold overall increase of the binding affinity for the oligopeptide Ac-Arg-Tyr-Phe($p$$NO_2$)-Chi-Chi-Chi-Arg-$NH_2$ ($K_d=2.6\times10^{-5}$ M) and afforded a 20-fold improvement for the oligopeptide Ac-Arg-Lys-Phe($p$$NO_2$)-Chi-Chi-Chi-Arg-$NH_2$ ($K_d=1.1\times10^{-5}$ M) due to the introduction of an additional positive charge. Realistically, addition of an extra positive charge did not result in a strong binding benefit, as the binding affinities of these two oligopeptides are in the same order of magnitude as the binding affinity of the oligopeptide Ac-Arg-Cbg-Cha-Chi-Chi-Tal-Arg-NH_2 (**B**; $K_d=3.5\times10^{-5}$ M), which was already optimized for the Ual-Sar sequence. From these results, we can conclude that the hydrophobic nature of small peptides is important for binding with dsDNA. These findings confirm the importance of hydrophobic interactions for DNA binding.

To further enhance the dsDNA-binding capacities of these oligopeptides, hybrid molecules were synthesized by coupling acridine units. With the synthesis of a new lysine-based acridine intercalating unit, Lys(Acr), the design and synthesis of peptide–acridine conjugates (PACs), peptide–bisacridine conjugates (PbACs), and dipeptide–acridine conjugates (DACs) became fairly straightforward. As such, three series of hybrid molecules binding DNA *via* a groove-binding/intercalation mechanism were evaluated for their dsDNA-binding affinity. Initially, three series of PACs were synthesized by coupling the new acridine unit to three different lead peptides, having slightly different binding affinities. Coupling of the acridine unit had a positive effect on the binding affinities of each lead peptide. However, the benefit was dependent on the initial binding affinity of the lead peptides. For all peptides, the benefit seems to be limited up to a maximum binding affinity in the range of 1 to 3×10^{-5} M. To evaluate whether coupling of a second acridine unit could further enhance the binding affinity, PbACs, having an intercalation/groove-binding/intercalation mechanism, were synthesized.

Coupling of an additional acridine unit did not lead to any significant binding benefit, indicating that a maximum benefit had already been reached with the introduction of one acridine unit. Finally, a third series of hybrid molecules were synthesized using actinomycin D as a model compound. The DACs having a groove-binding/intercalation/groove-binding mechanism were designed by a combination of lead peptides **A** and **B**. As such, three series of DACs were synthesized. Coupling of another groove-binding peptide could enhance the binding affinity with a factor 3 for both lead peptides in comparison with their parent PAC. The combi sequence, consisting of a combination of lead **A** and **B**, and the DACs derived from lead **B**, showed binding affinities in the low micromolar range up to 6.4×10^{-6} M for compound **2d**. These binding affinities are within the same range as the binding affinity of the known minor-groove binder *Hoechst 33258* for its target sequence. As such, the use of naturally occurring DNA binders as model compounds turned out to be a good strategy for the design of new dsDNA-binding ligands.

Experimental Part

General. MeCN for HPLC was purchased from *Biosolve* (NL-Valkenswaard) and water for HPLC purification was distilled twice. CH_2Cl_2, DMF, Ac_2O, and pyridine were obtained from *BDH* (UK-Poole). Piperidine, $EtN(i\text{-}Pr)_2$, CF_3COOH (TFA), diisopropylcarbodiimide (DIC), 1-hydroxybenzotriazole (HOBt), 1-methyl-1*H*-imidazole (NMI), acridine-9-carboxylic acid, and *O*-(1-azabenzotriazol-1-yl)-1,1,3,3-tetramethyluronium hexafluorophosphate (HATU) were supplied by *Acros Organics* (B-Geel). Anh. solvents were obtained as follows: CH_2Cl_2 was stored over CaH_2, refluxed, and distilled; pyridine and $EtN(i\text{-}Pr)_2$ were refluxed overnight in the presence of KOH and distilled. DMF was stored over activated molecular sieves (4 Å) for 3 d and was tested for absence of Me_2NH by the bromophenol test prior to use. *Rink* amide 4-methylbenzhydrylamine (MBHA) resin and [(1*H*-benzotriazol-1-yl)oxy]tris(pyrrolidin-1-yl)phosphonium hexafluorophosphate (PyBOP) were obtained from *Novabiochem* (CH-Läufelfingen). Oligonucleotides were purchased from *Eurogentec* (B-Seraing), or were prepared and purified in-house. The ethidium bromide soln. was obtained from *Bio-Rad* (B-Nazareth-Eke). Precoated *Sil G/UV 254* plates (*e.g.*, silica gel/TLC cards, *Fluka Chemika*, B-Bornem) were used for TLC, and spots were examined by UV light. Column chromatography (CC) was performed on *Acros* silica gel (60–200 μm, 6 nm; *Acros*, B-Geel). NMR Spectra were recorded on *Varian* 200- and 500-MHz instruments. Mass spectra were recorded with a quadrupole/orthogonal-acceleration time-of-flight (Q/oaTOF) tandem mass spectrometer (*qTof 2*, *Micromass*, UK-Manchester) equipped with a electrospray ionisator (ESI). The samples were injected in 1 : 1 with a flow rate of 3 μl/min. The masses were calculated with MassLynx 3.4 using the MaxEnt algorithm. Peptides were purified using reversed-phase HPLC equipped with a *L-6200A* intelligent pump (*Merck-Hitachi*, D-Darmstadt), a *Valco N6* injector, and a semipreparative *PLRP-S*^{R} column (250 mm × 9 mm, 100 Å, 15–20 μm; *Alltech*, B-Laarne). The spectra were detected with a *L-4200* UV/VIS detector (*Merck-Hitachi*, D-Darmstadt) coupled to a *Philips* recorder.

Amino Acids Used in the Synthesis of the Oligopeptides and Intercalator Conjugates. Amino acid building blocks N^{α}-Fmoc-β-(uracil-1-yl)-D-alanine (Ual), N^{α}-Fmoc-β-(thymin-1-yl)-D-alanine (Tal), N^{α}-Fmoc-β-(1,2,3,4-tetrahydro-2,4-dioxoquinazolin-3-yl)-D-alanine (Chi), and N^{α}-Fmoc-[(3-chlorobenzyl)-amino)]acetic acid (Cbg) were obtained according to the procedures reported in [5][7]. N^{α}-Fmoc-sarcosine (Sar), N^{α}-Fmoc-N^{ω}-2,2,5,7,8-pentamethylchromane-6-sulfonyl-L-arginine (Arg), N^{α}-Fmoc-N^{ε}-Boc-L-lysine (Lys), N^{α}-Fmoc-*O*-trityl-L-homoserine (Hse), N^{α}-Fmoc-cyclohexyl-L-alanine (Cha), N^{α}-Fmoc-*N*-(im)-trityl-L-histidine (His), N^{α}-Fmoc-β-thienyl-L-alanine (Thi), N^{α}-Fmoc-4-fluoro-L-phenylalanine (Phe(*p*F), and N^{α}-Fmoc-4-nitro-L-phenylalanine (Phe(*p*NO_2)) were obtained from *Novabiochem* (CH-Läufelfingen). N^{α}-Fmoc-D-alanine (Ala), N^{α}-Fmoc-L-leucine (Leu) and N^{α}-Fmoc-*O*-(*tert*-butyl)-L-tyrosine (Tyr) were obtained from *Advanced Chemtech* (UK-St George). N^{α}-Fmoc-L-Lysine-OH · HCl was purchased from *Fluka Chemika* (B-Bornem).

Synthesis of (2S)-6-{[(Acridin-9-yl)carbonyl]amino}-2-({[(9H-fluoren-9-yl)methoxy]carbonyl}amino)hexanoic Acid. EtN(i-Pr)$_2$ (940 µl, 5.38 mmol, 1.2 equiv.) was added to a suspension of acridine-9-carboxylic acid (1 g, 4.48 mmol, 1 equiv.) and HATU (1.7 g, 4.48 mmol, 1 equiv.) in 30 ml of anh. DMF, and the resulting soln. was stirred for 2 h at r.t. N^{α}-Fmoc-Lys-OH · HCl (1.45 g, 3.58 mmol, 0.8 equiv.) dissolved in 7 ml of anh. DMF and neutralized with EtN(i-Pr)$_2$ (623 µl, 3.58 mmol, 0.8 equiv.) was added to the mixture, and the mixture was stirred overnight at r.t. After evaporation, the remaining residue was dissolved in H_2O and acidified to pH 2 with 2N HCl. After filtration, the reaction product was further purified by CC (silica gel; CH_2Cl_2/MeOH/glacial AcOH 100 : 0 : 0.1 to 95 : 5 : 0.1). The title compound was obtained as a yellow amorphous solid in 71% yield. R_f (CH_2Cl_2/MeOH/glacial AcOH 95 : 5 : 0.1) 0.45. ^{1}H-NMR (200 MHz, (D_6)DMSO): 1.24–1.40 (*m*, 2 H–C(δ) (Lys)); 1.40–1.57 (*m*, 2 H–C(δ) (Lys)); 1.57–1.73 (*m*, 2 H–C(β) (Lys)); 3.40–3.56 (*m*, 2 H–C(ε) (Lys)); 3.9 (*m*, 2 H–C(α) (Lys)); 4.18–4.32 (*m*, CH_2O(C=O) and H–C(9) of Fmoc); 5.75 (*d*, N^{α}H (Lys)); 7.27–8.22 (16 arom. H), 9.0 (*t*, N^{ε}H (Lys)). ^{13}C-NMR (200 MHz, (D_6)DMSO): 23.1 (C(γ) (Lys)); 28.8 (C(δ) (Lys)); 30.5 (C(β) (Lys)); 38.2 (C(ε) (Lys)); 46.7 (*C*CH_2O(C=O)N of Fmoc); 54.0 (C(α) (Lys)); 65.7 (*C*H_2O(C=O)N of Fmoc); 120.3, 121.0. 125.5, 125.8, 126.95, 127.3, 127.9, 129.5, 130.8, 140.9, 142.7, 144.0, 148.4 (arom. C); 156.5 (O(C=O)N of Fmoc); 166.14 ((C=O)N of Acr); 174.28 ((C=O)OH of Lys). HR-MS (ESI/TOF+): 596.2179 ($[M+Na]^+$; calc. 596.2161), 574.2356 ($[M+H]^+$, $C_{35}H_{31}N_3O_5^+$; calc. 574.2342).

Solid-Phase Synthesis of the Amino Acid Substituted Oligopeptides. The amino acid building blocks were coupled with classical coupling reagents for peptide-bond formation and Fmoc-substituted amino acids. Peptide-bond formation was performed with a mixture of DIC (4 equiv.), HOBt (4 equiv.), PyBOP (2 equiv.), EtN(i-Pr)$_2$ (4 equiv.), and the Fmoc-substituted amino acids (4 equiv. with respect to the available amines on the *Rink* amide MBHA resin) in DMF. Deprotection of the Fmoc-protected solid-support was carried out by shaking the resin with 20% piperidine in DMF for 15 min. The mixture of the Fmoc-substituted amino acid and the coupling reagents in DMF was then added to the amino-functionalized resin. The reaction vessel was shaken for 16 h. Then, the mixture was filtered, and the beads were washed five times with DMF, three times with CH_2Cl_2, and twice with Et_2O. The beads were dried *in vacuo*, and the Fmoc-substitution level was determined by dissolving an accurately measured quantity of resin (± 10 mg) in 20% piperidine in DMF (exactly 25.0 ml). After 10 min, the absorbance was measured at 300 nm *vs.* a 20% soln. of piperidine in DMF as blank, allowing calculation of the substitution level ($\varepsilon = 7500$). When the coupling yield was satisfactory, the beads were prepared for coupling the next amino acid. The residual amines were capped (acetylated) by shaking the resin with a mixture of pyridine/Ac_2O/NMI 4 : 1 : 0.5 in order to avoid formation of deletion peptides. After shaking for 10 min, the resins were washed three times with DMF, three times with CH_2Cl_2, three times with DMF, and once with 20% piperidine in DMF, before the Fmoc protecting groups were removed by shaking the resins for 15 min in 20% piperidine in DMF to allow coupling of the next Fmoc-substituted amino acid building block. This synthetic cycle was carried out until the complete oligopeptide sequence was assembled on the solid-support. After the last assembly cycle, the resin-bound oligopeptide sequence was Fmoc-deprotected and acetylated. Since all the side-chain protecting groups were acid labile, the oligopeptides were deprotected and cleaved from the resins by shaking the beads with TFA/H_2O/thioanisole 95 : 5 : 5 for 2 h. After 2 h, the resins were filtered, and the filtrate was immediately precipitated with ^{i}Pr$_2$O at −70°. The white cloudy suspension obtained was centrifuged for 10 min at 9000 rpm. After removal of the supernatants, the remaining pellet was washed with fresh ^{i}Pr$_2$O at −70°. The white cloudy suspension obtained was centrifuged for 10 min at 9000 rpm. After removal of the supernatants, the remaining pellet was dried *in vacuo* and dissolved in H_2O/MeCN 9 : 1. Finally, the oligopeptides were purified by reversed-phase semi-prep. HPLC with H_2O/MeCN/TFA 95 : 5 : 0.1 to 20 : 80 : 0.1 over 45 min with UV detection at 254 nm. After purification, the pure peptide samples were frozen and lyophilized overnight. Characterization of the oligopeptides was performed by mass spectrometry (*Table 7*). After characterization, the peptides were dissolved in DMSO in an appropriate concentration for soln.-phase screening.

Solid-Phase Synthesis of the Oligopeptide–Acridine Conjugates. Solid-phase synthesis was performed in accordance to the protocols as pointed out above. (*2S*)-6-{[(acridin-9-yl)carbonyl]amino}-2-({[(9*H*-fluoren-9-yl)methoxy]carbonyl}amino)hexanoic acid (4 equiv.) was coupled by using a mixture of HOBT (4 equiv.), PyBOP (2 equiv.), DIC (4 equiv.), and EtN(i-Pr)$_2$ (4 equiv.) in anh. DMF. After completion of the

Table 7. *Calculated and Observed Molecular Masses of the Different Synthesized Oligopeptide Sequences as Determined by Mass Spectrometry.* Masses were obtained as $[M+2\,H]^{2+}$.

Oligopeptide sequence	M_r	
	calc.	found
Ac-Arg-Ual-Sar-Lum^3-Lum^3-Lum^3-Arg-NH_2 [16]	662.2440	662.2410
Sar Substitutions:		
Ac-Arg-Ual-Hse-Chi-Chi-Chi-Arg-NH_2	674.2645	674.2700
Ac-Arg-Ual-Leu-Chi-Chi-Chi-Arg-NH_2	680.7866	680.7919
Ac-Arg-Ual-Ala-Chi-Chi-Chi-Arg-NH_2	659.2592	659.2651
Ac-Arg-Ual-His-Chi-Chi-Chi-Arg-NH_2	692.2701	692.2767
Ac-Arg-Ual-Tyr-Chi-Chi-Chi-Arg-NH_2	705.2684	705.2808
Ac-Arg-Ual-Thi-Chi-Chi-Chi-Arg-NH_2	700.2530	700.2606
Ac-Arg-Ual-Phe(*p*F)-Chi-Chi-Chi-Arg-NH_2	706.2701	706.2773
Ac-Arg-Ual-Phe(*p*NO_2)-Chi-Chi-Chi-Arg-NH_2	719.7674	719.7767
Ual Substitutions:		
Ac-Arg-His-Phe(*p*NO_2)-Chi-Chi-Chi-Arg-NH_2	697.7724	697.7794
Ac-Arg-Tyr-Phe(*p*NO_2)-Chi-Chi-Chi-Arg-NH_2	710.7747	710.7827
Ac-Arg-Lys-Phe(*p*NO_2)-Chi-Chi-Chi-Arg-NH_2	693.2944	693.2977

Table 8. *Calculated and Observed Molecular Masses of the Different Synthesized Oligopeptide–Acridine Conjugates as Determined by Mass Spectrometry.* Masses were obtained as $[M+2\,H]^{2+}$.

Oligopeptide–acridine conjugate sequence	M_r	
	calc.	found
Ac-Lys(Acr)-Arg-Ual-Sar-Chi-Chi-Chi-Arg-NH_2	825.8330	825.8384
Ac-Lys(Acr)-Gly-Arg-Ual-Sar-Chi-Chi-Chi-Arg-NH_2	854.3438	854.3460
Ac-Lys(Acr)-β-Ala-Arg-Ual-Sar-Chi-Chi-Chi-Arg-NH_2	861.3516	861.3578
Ac-Lys(Acr)-Gly-Gly-Arg-Ual-Sar-Chi-Chi-Chi-Arg-NH_2	882.8545	882.8622
Ac-Lys(Acr)-β-Ala-Gly-Arg-Ual-Sar-Chi-Chi-Chi-Arg-NH_2	889.8623	889.8704
Ac-Lys(Acr)-GABA-Arg-Ual-Sar-Chi-Chi-Chi-Arg-NH_2	868.3594	868.3630
Ac-Lys(Acr)-6-Ahx-Arg-Ual-Sar-Chi-Chi-Chi-Arg-NH_2	882.3751	882.3803
Ac-Lys(Acr)-Gly-Arg-Cbg-Cha-Chi-Chi-Tal-Arg-NH_2	877.3733	877.3810
Ac-Lys(Acr)-β-Ala-Arg-Cbg-Cha-Chi-Chi-Tal-Arg-NH_2	884.3811	884.3870
Ac-Lys(Acr)-Gly-Gly-Arg-Cbg-Cha-Chi-Chi-Tal-Arg-NH_2	905.8840	905.8904
Ac-Lys(Acr)-β-Ala-Gly-Arg-Cbg-Cha-Chi-Chi-Tal-Arg-NH_2	912.8976	912.8918
Ac-Lys(Acr)-6-Ahx-Arg-Cbg-Cha-Chi-Chi-Tal-Arg-NH_2	905.4046	905.4130
Ac-Lys(Acr)-Arg-Ual-Phe(*p*NO_2)-Chi-Chi-Chi-Arg-NH_2	859.8642	859.8645
Ac-Lys(Acr)-Gly-Arg-Ual-Phe(*p*NO_2)-Chi-Chi-Chi-Arg-NH_2	888.3751	888.3771
Ac-Lys(Acr)-β-Ala-Arg-Ual-Phe(*p*NO_2)-Chi-Chi-Chi-Arg-NH_2	895.3813	895.3830
Ac-Lys(Acr)-6-Ahx-Arg-Ual-Phe(*p*NO_2)-Chi-Chi-Chi-Arg-NH_2	916.4064	916.4094

synthesis cycle, the PACs were cleaved from the solid-support, purified with reversed-phase HPLC, and characterized by mass spectrometry (*Table 8*). After characterization, the PACs were dissolved in DMSO in an appropriate concentration for soln.-phase screening.

Solid-Phase Synthesis of the Oligopeptide–Bisacridine Conjugates and Preparation for Soln.-Phase Screening. Solid-phase synthesis of the oligopeptide–bisacridine conjugates was performed as depicted in *Scheme 2.* Coupling of (*2S*)-6-{[(acridin-9-yl)carbonyl]amino}-2-({[(9*H*-fluoren-9-yl)methoxy]-carbonyl}amino)hexanoic acid was performed with a mixture of HOBt (4 equiv.), PyBOP (2 equiv.),

DIC (4 equiv.), EtN(i-Pr)$_2$ (4 equiv.), and the Fmoc-substituted amino acid (4 equiv. with respect to the available amines on the *Rink* amide MBHA solid support) in anh. DMF. The NH_2-terminal acridine-9-carboxylic acid unit was coupled with a mixture of HATU (4 equiv.), EtN(i-Pr)$_2$ (4 equiv.), and 4 equiv. of the heteropolyaromatic acridine moiety in anh. DMF. After completion of the synthesis cycle, the oligopeptide–bisacridine conjugates were cleaved from the solid-support, purified with reversed-phase HPLC, and characterized by mass spectrometry (*Table 9*). After characterization, the PbACs were dissolved in DMSO in an appropriate concentration for soln.-phase screening.

Table 9. *Calculated and Observed Molecular Masses of the Different Synthesized Oligopeptide–Bisacridine Conjugates as Determined by Mass Spectrometry.* Masses were obtained as $[M+2\,H]^{2+}$.

Oligopeptide–acridine conjugate sequence	M_r	
	calc.	found
Acr-Gly-Arg-Ual-Sar-Chi-Chi-Chi-Arg-Lys(Acr)-NH_2	935.8649	935.8668
Acr-Gly-Arg-Ual-Sar-Chi-Chi-Chi-Arg-Gly-Lys(Acr)-NH_2	964.3756	964.3744
Acr-Gly-Arg-Ual-Sar-Chi-Chi-Chi-Arg-β-Ala-Lys(Acr)-NH_2	971.3834	971.3838
Acr-Gly-Arg-Ual-Sar-Chi-Chi-Chi-Arg-Gly-Gly-Lys(Acr)-NH_2	992.8863	992.8871
Acr-Gly-Arg-Ual-Sar-Chi-Chi-Chi-Arg-β-Ala-Gly-Lys(Acr)-NH_2	999.8941	999.8943
Acr-Gly-Arg-Ual-Sar-Chi-Chi-Chi-Arg-GABA-Lys(Acr)-NH_2	978.3913	978.3916
Acr-Gly-Arg-Ual-Sar-Chi-Chi-Chi-Arg-6-Ahx-Lys(Acr)-NH_2	992.4088	992.4069

Solid-Phase Synthesis of the Dipeptide–Acridine Conjugates and Preparation for Soln.-Phase Screening. Solid-phase synthesis of the dipeptide–acridine conjugates was performed as depicted in *Scheme 3*.

Amino acid building blocks of the second, reversed oligopeptide sequence were coupled with a mixture of HOBt (4 equiv.), PyBOP (2 equiv.), DIC (4 equiv.), EtN(i-Pr)$_2$ (4 equiv.), and the Fmoc-substituted amino acids (4 equiv. with respect to the available amines on the *Rink* amide MBHA resin) in anh. DMF. Amino acids Cha, Cbg, and Arg2 of the second peptide sequence had to be coupled twice in order to achieve a complete coupling as determined by the *Kaiser* test. After completion of the synthesis cycle, the DACs were cleaved from the solid-support, purified with reversed phase HPLC, and characterized by mass spectrometry (*Table 10*). After characterization, the DACs were dissolved in DMSO in an appropriate concentration for soln.-phase screening.

Soln.-Phase Screening: Ethidium Bromide Displacement Experiments (FID). The FID experiments were performed with the 14-bp semi palindromic dsDNA sequence (5′-AGATTGTGCAATGT-3′) as target. Each well of a *Costar* black 96-well plate was loaded with 2 µl of a 50 µM dsDNA soln. (14 µM in DNA bp final concentration), 2 µl of a 0.35 mM EtBr soln. (7 µM final concentration), and a varying volume of oligopeptide to obtain the necessary concentrations. The appropriate volume of a *Tris*/NaCl buffer (10 mM *Tris*/10 mM NaCl pH, 7.4) was added to obtain a total volume of 100 µl per well. Before adding the DNA into the wells, it was rendered double-stranded by placing equal amounts of the two complementary strands for 3 min at 80°, at r.t. for 5 min and at 4° for 20 min. After incubation at r.t. for 30 min, each well was read on a *FL600 Microplate Fluorescence* reader (*Biotek*, Winooski, USA), with 530/25 nm as excitation wavelength and 590/35 nm as emission-detection wavelength. Two control wells (no agent = 100% fluorescence, no DNA = 0% fluorescence) were used per 12 samples. Fluorescence readings are reported as % fluorescence relative to the control wells. Generally, each plate was read three times to calculate average values.

Determination of Apparent Dissociation Constants (K_d). Apparent dissociation constants were determined using the FID assay as described above using oligopeptide or oligopeptide–intercalator (PAC, PbAC, or DAC) concentrations ranging from 1 to 100 µM, depending on their dsDNA-binding affinities, with concentration increments of 1 or 2 µM final oligopeptide concentration. The K_d value was determined as the concentration at which the fluorescence intensity was decreased to 50% of the initial value.

Table 10. *Calculated and Observed Molecular Masses of the Different Synthesized Dipeptide–Acridine Conjugates as Determined by Mass Spectrometry.* Masses were obtained as $[M+3\,H]^{3+}$.

Dipeptide–acridine conjugate sequence	M_r	
	calc.	found
Derived from lead **A**[a]):		
Ac-Arg-Chi-Chi-Chi-Sar-Ual-Arg-Gly-Ref[a]	1026.7509	1026.7589
Ac-Arg-Chi-Chi-Chi-Sar-Ual-Arg-β-Ala-Ref[a]	1032.0567	1032.0999
Ac-Arg-Chi-Chi-Chi-Sar-Ual-Arg-Gly-Gly-Ref[a]	1045.7581	1045.7653
Ac-Arg-Chi-Chi-Chi-Sar-Ual-Arg-Gly-β-Ala-Ref[a]	1050.4300	1050.4385
Ac-Arg-Chi-Chi-Chi-Sar-Ual-Arg-6-Ahx-Ref[a]	1045.4385	1045.4456
Combi-sequence[b]):		
Ac-Arg-Tal-Chi-Chi-Cha-Cbg-Arg-Gly-Ref[b]	1042.1052	1042.1089
Derived from lead **B**[c]):		
Ac-Arg-Tal-Chi-Chi-Cha-Cbg-Arg-Gly-Ref[c]	1057.4535	1057.4645
Ac-Arg-Tal-Chi-Chi-Cha-Cbg-Arg-Gly-Gly-Ref[c]	1076.4640	1076.4712
Ac-Arg-Tal-Chi-Chi-Cha-Cbg-Arg-β-Ala-Gly-Ref[c]	1081.1359	1081.1414
Ac-Arg-Tal-Chi-Chi-Cha-Cbg-Arg-6-Ahx-Ref[c]	1076.1444	1076.1503
Ac-Arg-Tal-Chi-Chi-Cha-Cbg-Arg-Gaba-Gly-Ref[c]	1066.8007	1066.8069

[a]) Ref[a] = -Lys(acr)-6-Ahx-Arg-Ual-Sar-Chi-Chi-Chi-Arg-NH_2. [b]) Ref[b] = -Lys(acr)-6-Ahx-Arg-Ual-Sar-Chi-Chi-Chi-Arg-NH_2. [c]) Ref[c] = -Lys(Acr)-6-Ahx-Arg-Cbg-Cha-Chi-Chi-Tal-Arg-NH_2.

F. B. would like to thank *IWT* for financial support. The authors are very grateful to *K. U. Leuven* (GOA/2002/13) for financial support and to *Chantal Biernaux* for editorial help.

REFERENCES

[1] A. M. Caamaño, M. E. Vazquez, J. Martinez-Costas, L. Castedo, J. L. Mascareñas, *Angew. Chem., Int. Ed.* **2000**, *39*, 3104.
[2] P. B. Dervan, *Bioorg. Med. Chem.* **2001**, *9*, 2215.
[3] B. A. Janowski, K. Kaihatsu, K. E. Huffman, J. C. Schwartz, R. Ram, D. Hardy, C. R. Mendelson, D. R. Corey, *Nature, Chem. Biol.* **2005**, *1*, 210.
[4] P. E. Nielsen, *Curr. Opin. Mol. Ther.* **2000**, *28*, 3332.
[5] P. Chaltin, E. Lescrinier, T. Lescrinier, J. Rozenski, J. Hendrix, R. Rosemeyer, R. Busson, A. Van Aerschot, P. Herdewijn, *Helv. Chim. Acta*. **2002**, *85*, 2258.
[6] P. Chaltin, F. Borgions, A. Van Aerschot, P. Herdewijn, *Bioorg. Med. Chem. Lett.* **2003**, *13*, 47.
[7] Z. Zhang, P. Chaltin, A. Van Aerschot, J. Lacey, J. Rozenski, R. Busson, P. Herdewijn, *Bioorg. Med. Chem.* **2002**, *10*, 3401.
[8] D. L. Boger, B. E. Fink, S. R. Brunette, C. T. Winston, M. P. Hendrick, *J. Am. Chem. Soc.* **2001**, *123*, 5878.
[9] A. R. Urbach, P. B. Dervan, *Proc. Natl. Acad. Sci. U.S.A.* **2001**, *98*, 4343.
[10] C. Bailly, J. P. Hénichart, *Bioconjugate Chem.* **1991**, *2*, 379.
[11] X. L. Xang, A. H.-J. Wang, *Pharmacol. Ther.* **1999**, *83*, 181.
[12] H. M. Sobell, S. C. Jain, *J. Mol. Biol.* **1972**, *68*, 21.
[13] C. Bailly, B. Chaires, *Bioconjugate Chem.* **1998**, *9*, 513.
[14] J. P. Hénichart, M. J. Waring, J. F. Riou, W. A. Denny, C. Bailly, *Mol. Pharmacol.* **1997**, *51*, 448.
[15] E. J. Fechter, P. B. Dervan, *J. Am. Chem. Soc.* **2003**, *125*, 8476.
[16] P. Chaltin, F. Borgions, J. Rozenski, A. Van Aerschot, P. Herdewijn, *Helv. Chim. Acta* **2003**, *86*, 533.
[17] P. Roepstorff, J. Fohlman, *Biomed. Mass Spectrom.* **1984**, *11*, 601.

Received March 20, 2006